

RESEARCH ARTICLE

On the hydrography of Denmark Strait

10.1002/2016JC012007

Key Points:

- The signature of upstream flow components is distinctly visible in composite hydrographic sections across the Denmark Strait sill
- The relative contributions of source waters to the Denmark Strait overflow are determined using an end-member analysis
- Weakly stratified boluses, composed primarily of Arctic-Origin Water, are found in the overflow in 41% of the hydrographic sections

Correspondence to:

D. Mastropole,
dmastropole@whoi.edu

Citation:

Mastropole, D., R. S. Pickart, H. Valdimarsson, K. Våge, K. Jochumsen, and J. Girton (2017), On the hydrography of Denmark Strait, *J. Geophys. Res. Oceans*, 122, 306–321, doi:10.1002/2016JC012007.

Received 31 MAY 2016

Accepted 28 NOV 2016

Accepted article online 20 DEC 2016

Published online 20 JAN 2017

Dana Mastropole ¹, Robert S. Pickart¹, Héðinn Valdimarsson², Kjetil Våge ³, Kerstin Jochumsen⁴, and James Girton ⁵

¹Department of Physical Oceanography, Woods Hole Oceanographic Institution, Woods Hole, Massachusetts, USA,

²Marine Environment Section, Marine Research Institute, Reykjavík, Iceland, ³Bjerknes Center for Climate Research, University of Bergen, Bergen, Norway, ⁴Institute of Oceanography, Universität Hamburg, Hamburg, Germany, ⁵Applied Physics Laboratory, University of Washington, Seattle, Washington, USA

Abstract Using 111 shipboard hydrographic sections across Denmark Strait occupied between 1990 and 2012, we characterize the mean conditions at the sill, quantify the water mass constituents, and describe the dominant features of the Denmark Strait Overflow Water (DSOW). The mean vertical sections of temperature, salinity, and density reveal the presence of circulation components found upstream of the sill, in particular the shelfbreak East Greenland Current (EGC) and the separated EGC. These correspond to hydrographic fronts consistent with surface-intensified southward flow. Deeper in the water column the isopycnals slope oppositely, indicative of bottom-intensified flow of DSOW. An end-member analysis indicates that the deepest part of Denmark Strait is dominated by Arctic-Origin Water with only small amounts of Atlantic-Origin Water. On the western side of the strait, the overflow water is a mixture of both constituents, with a contribution from Polar Surface Water. Weakly stratified “boluses” of dense water are present in 41% of the occupations, revealing that this is a common configuration of DSOW. The bolus water is primarily Arctic-Origin Water and constitutes the densest portion of the overflow. The boluses have become warmer and saltier over the 22 year record, which can be explained by changes in end-member properties and their relative contributions to bolus composition.

1. Introduction

Dense water formed in the Nordic Seas spills over the Greenland-Scotland Ridge as overflow plumes, feeding the lower limb of the Atlantic Meridional Overturning Circulation (AMOC). The largest of these is the Denmark Strait Overflow Water (DSOW), which supplies approximately half of the dense water to the headwaters of the Deep Western Boundary Current [Dickson *et al.*, 2008]. As this water exits the Iceland Sea, it flows through both a lateral constriction and shoaling topography before descending the continental slope of the northern Irminger Sea. Consequently, hydraulic control is believed to play a role in dictating the transport of the DSOW [Nikolopoulos, 2003]. Immediately south of the sill the overflow water undergoes strong entrainment, which is related to the density of the overflowing plume [Price and O’Neil Baringer, 1994]. Therefore, it is important to understand the hydrographic character of the DSOW and the manner in which it passes over the sill.

DSOW approaches the sill via three pathways: the shelfbreak East Greenland Current (shelfbreak EGC), the separated East Greenland Current (separated EGC), and the North Icelandic Jet (NIJ) (Figure 1). Mauritzen [1996] proposed the first pathway in which water within the Norwegian Atlantic Current cools and densifies as it flows around the perimeter of the Nordic Seas. A portion of this water retroreflects south of Fram Strait and joins the shelfbreak EGC flowing southward toward Denmark Strait [Paquette *et al.*, 1985]. It has recently been shown that, in the vicinity of the Blossville Basin, the current bifurcates [Våge *et al.*, 2013] and nearly half of the Atlantic-Origin Overflow Water crosses the basin to the base of the Iceland slope [Harden *et al.*, 2016]. This separated branch of the EGC constitutes the second dense water pathway approaching Denmark Strait.

The third overflow pathway is the NIJ, an equatorward flowing jet centered near the 650 m isobath on the Iceland slope. Jónsson and Valdimarsson [2004] first reported the existence of the jet, and subsequent field studies have revealed that it contributes about a third of the overflow water transport at the sill, including the densest component [Våge *et al.*, 2013; Harden *et al.*, 2016]. Våge *et al.* [2011] hypothesized that the NIJ is

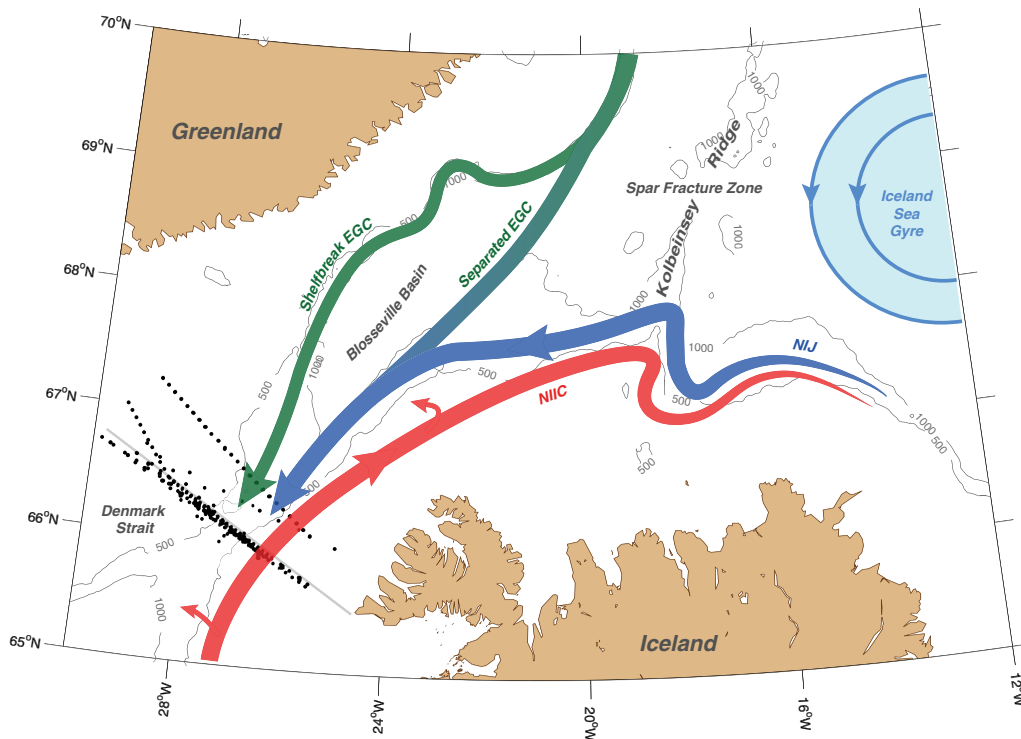


Figure 1. Schematic of the currents flowing through Denmark Strait and various place names, after *Våge et al.* [2013]. The Látrabjarg line, located near the sill, is drawn in gray. The black dots are the CTD stations comprising the 111 shipboard transects used in the study (the majority of which are along the Látrabjarg line). The 500 and 1000 m isobaths are contoured in gray. EGC = East Greenland Current; NIJ = North Icelandic Jet; NIIC = North Icelandic Irminger Current.

the lower limb of a local overturning loop north of Iceland, whose upper limb is the warm and salty North Icelandic Irminger Current (NIIC). According to their model, the NIIC is believed to shed eddies which transport water into the interior. The water is then made dense due to heat loss in the winter, and the dense product, known as Arctic-Origin Overflow Water, returns to the boundary where it sinks and forms the NIJ [*Våge et al.*, 2011].

Mooring time series at the sill have shown that there is no significant seasonal signal of the overflow, and only weak interannual variability has been detected [*Dickson and Brown*, 1994; *Jónsson*, 1999; *Jochumsen et al.*, 2012]. However, numerous observational studies through the years have revealed large fluctuations in the structure of the DSOW on short time scales of a few days. Using hydrographic sections south of Denmark Strait, *Cooper* [1955] first attributed this variability to the transit of large, cold, intermittent lenses of Norwegian Sea Water called boluses. The existence of such boluses was later supported by the work of *Worthington* [1969], who observed periods of cold, fast currents interspersed with warm, slow currents in mooring data close to the sill. Since then, boluses have been identified in various observational data sets and in numerical models as well [*Spall and Price*, 1998; *Rudels et al.*, 1999; *Girton and Stanford*, 2003; *Käse et al.*, 2003; *Magaldi et al.*, 2011; *Koszalka et al.*, 2013].

Several theories postulate the formation of boluses and their frequency of passage. *Smith* [1976] hypothesized that boluses form due to baroclinic instability of the overflow. It was demonstrated that the dominant period of variability in current meter records matched that of the most unstable baroclinic wave in a linear, idealized flow in Denmark Strait. An alternate theory was later proposed after the discovery of a weakly stratified southward-flowing current in Denmark Strait [*Fristedt et al.*, 1999]. The current was shown to have unstable growth rates comparable to the baroclinic wave proposed by *Smith* [1976], that could be responsible for fluctuations in the overflow. Other studies have found that the initial velocity, width, and density of the overflow plume, along with the steepness of the topography, influence the characteristics of the boluses [*Jungclauss and Backhaus*, 1994; *Jiang and Garwood*, 1996; *Krauss and Käse*, 1998; *Shi et al.*, 2001].

The presence of such lenses of overflow water has implications for regional and global circulation. Their low temperatures may help set the properties of North Atlantic Deep Water [Price and O'Neil Baringer, 1994], and their presence is thought to increase the transport of the overflow at the sill [Price and O'Neil Baringer, 1994; Koszalka et al., 2013]. Furthermore, there is evidence from mooring data, satellite observations, modeling studies, and laboratory experiments that boluses spin up cyclones south of the sill [Smith, 1975; Bruce, 1995; Krauss, 1996; Jiang and Garwood, 1996; Krauss and Käse, 1998; Spall and Price, 1998; Käse and Oschlies, 2000; Käse et al., 2003; Magaldi et al., 2011; von Appen et al., 2014a]. In turn, the cyclones entrain water downstream of the sill and contribute to the mixing and modification of DSOW.

Our study seeks to characterize the hydrographic structure of the different water masses at the Denmark Strait sill, with particular focus on the DSOW before it descends into the Irminger Basin. While there are well-defined flow pathways in the northern part of the strait, it is presently unknown if these branches are distinguishable at the sill and how they might interact due to the shoaling topography and lateral constriction. Synoptic transects across the sill are often difficult to interpret because of the complex water mass structure at any given time. For this reason, we have gathered all known shipboard hydrographic crossings in the vicinity of the sill, collected between 1990 and 2012, in order to give us a better chance of characterizing the dominant signals. We begin the study by constructing mean sections of hydrographic variables and connecting the features to known water masses and currents upstream of Denmark Strait. We then use an objective definition to identify boluses in the individual sections, and characterize their structure, size, location, and relationship to the surrounding DSOW in the strait. Lastly, we discuss long-term trends in the hydrographic characteristics and water mass constituents of the bolus water.

2. Data and Methods

2.1. Shipboard Measurements in Denmark Strait

We use conductivity-temperature-depth (CTD) data from 111 shipboard transects occupied in the vicinity of the Denmark Strait sill between March 1990 and August 2012 (Figures 1 and 2). Pertinent information for each section is contained in Table 1. Most of the transects were carried out by the Marine Research Institute of Iceland as part of their quarterly surveys or as contributions to larger programs such as the World Ocean Circulation Experiment (Nordic-WOCE) and the Variability of Exchanges in the Northern Seas (VEINS) program. Of the 111 sections, 88 were occupied precisely along the Látrabjarg line (which is the Icelandic standard section that crosses the sill) and 23 sections were done in the vicinity of the line. For the purposes of this study, the Látrabjarg line was adjusted slightly. In particular, it was defined using five occupations across the strait that extended well onto the Greenland shelf and included bathymetric data. A regression line was created (the gray line in Figure 1) and the echosounder data were despiked and smoothed along the line (Figure 3). We have defined the trough as the region between the Greenland and Iceland shelf-breaks, which contains a ledge on its western side (these features are marked in Figure 3).

The CTD data were obtained directly from the individual institutions (Table 1) each of which have their own processing and calibration procedures. A total of 1136 CTD stations were considered. We applied an additional level of quality control to each profile by first filtering out small-scale fluctuations using a fifth-order Butterworth filter (cutoff of 7 m) and then removing density inversions. This was done by manually adjusting the corresponding values of temperature and salinity to make the profile stably stratified at the depth in question (these adjustments were straightforward and only 0.2% of the data were corrected in this way). The location of each station was then projected normally onto the regression line (hereafter referred to as the Látrabjarg line). Only stations within 75 km of the line were considered, 90% of which fall within 5 km (Figure 1). Some of the CTD stations were further adjusted horizontally by a maximum of 2 km (a distance smaller than the horizontal grid spacing of the standard grid, see below) to better align the depth of the station with the bottom depth along the regression line. This is akin to projecting some of the stations (particularly those farther away from the Látrabjarg line) along the isobaths.

To carry out the analysis, we then gridded each section along the regression line to create vertical property sections. This process is explained in detail in Mastropole [2015], but is briefly described here. First, using a Laplacian spline interpolator with tension [Smith and Wessel, 1990], the data for each occupation were interpolated onto a low, medium, or high resolution grid according to the original station spacing (which ranged from 6 km to 25 km). A hybrid interpolation technique, similar to the one employed by Harden et al. [2016],

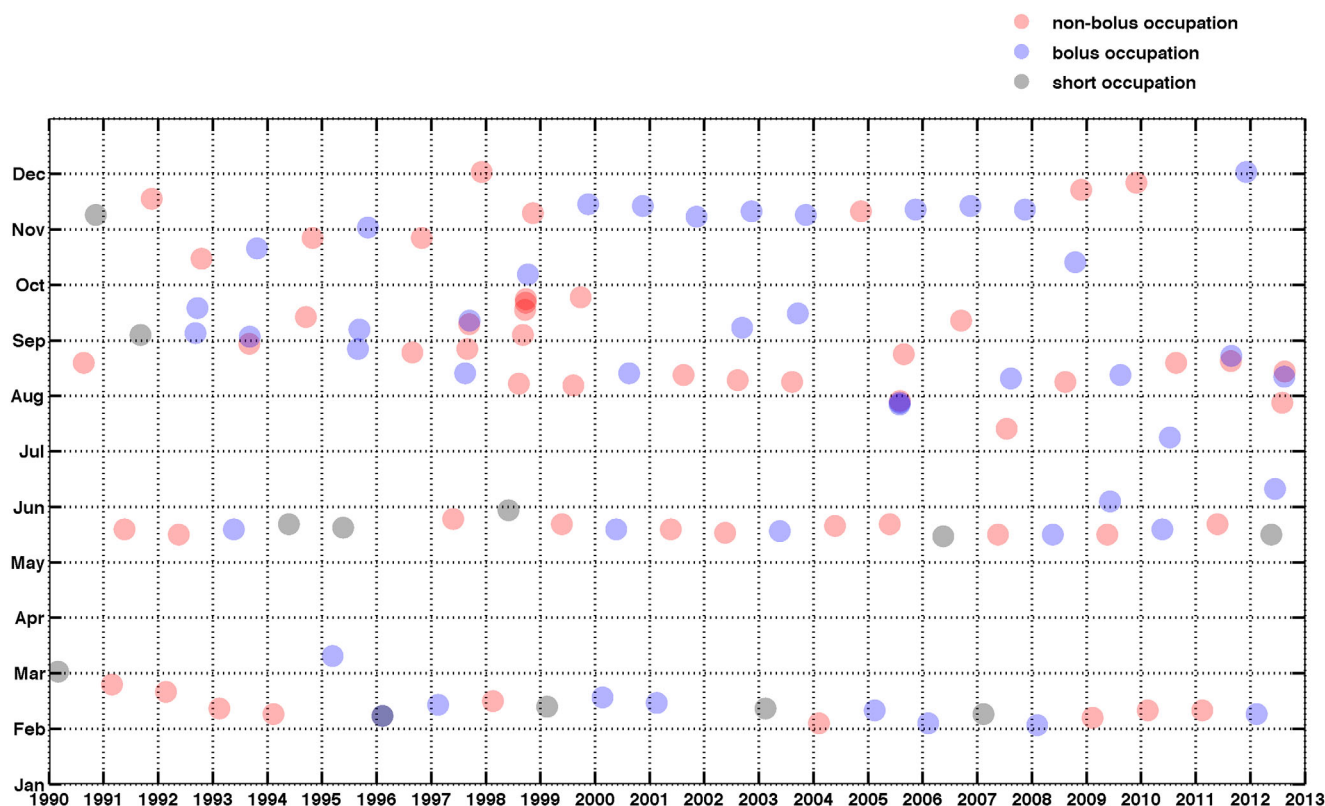


Figure 2. The months and years that the hydrographic transects were occupied. The symbol's opacity signifies the number of occupations conducted within a particular month. Blue color indicates that a bolus was present in the section, while red color indicates the absence of such a feature. A nonbolus occupation does not imply there was no overflow water present. Occupations that did not fully resolve the region where boluses are typically found are indicated by gray.

was applied where interpolation in depth space was done near the surface (potential density $\leq 27.5 \text{ kg/m}^3$) and interpolation in density space was done near the bottom (potential density $\geq 27.70 \text{ kg/m}^3$). A weighted average—where the weights are computed as a linear function of distance from one isopycnal to the other—was used for the region between the two isopycnals in question. After the interpolation in density space, the gridded hydrographic fields were transformed back into depth space. A subset of 30 occupations were interpolated entirely in depth space to preserve particular features at the bottom of the trough. Finally, those occupations with low and medium resolution were regridded onto a standard high-resolution grid of 2.5 km by 10 m. This way all of the occupations were on an identical grid, which facilitated the subsequent analysis. We note that the gridded density was smoothed further using a Laplacian algorithm to remove a small bit of noise. All temperatures and densities reported in the paper are potential values referenced to the sea surface.

2.2. Historical Hydrographic Data

A database of shipboard CTD measurements and Argo profiles in the Nordic Seas, encompassing the region between $65^\circ\text{N} - 80^\circ\text{N}$ and $8^\circ\text{W} - 28^\circ\text{W}$, is used to investigate the origin of the water passing through Denmark Strait and to construct three of the water mass end-members presented in section 3.2. The initial version of the database is described in detail in *Våge et al.* [2013], and the updated version is described in *Våge et al.* [2015]. HydroBase3, a hydrographic database containing shipboard CTD measurements and Argo profiles over the entire North Atlantic Ocean, was used for calculating the water mass end-member in the Irminger Sea. More information about the principle sources of data in HydroBase3 can be found at <http://www.whoi.edu/science/PO/hydrobase/php/index.php>.

2.3. Defining Boluses of Overflow Water in the Synoptic Sections

Boluses are large lenses of weakly stratified overflow water that are periodically present in Denmark Strait. For the present study, we identify them according to their homogeneity in water properties and their size.

Table 1. Information for the 111 Shipboard Hydrographic Sections Used in the Study, After von Appen et al. [2014b]^a

Abbreviation	Ship Name	Country			
<i>(a)</i>					
A	Árni Friðriksson	Iceland			
AR	Aranda	Finland			
B	Bjarni Sæmundsson	Iceland			
D	Discovery	United Kingdom			
JR	James Clark Ross	United Kingdom			
KN	Knorr	United States			
M	Meteor	Germany			
MSM	Maria S. Merian	Germany			
P	Poseidon	Germany			
PS	Polarstern	Germany			
Date	Cruise	Date	Cruise	Date	Cruise
<i>(b)</i>					
Mar 1990	B-03-1990	May 1998	B-06-1998	Aug 2005	P-327
Aug 1990	B-13-1990	Aug 1998	A-09-1998	Aug 2005	P-327
Nov 1990	B-17-1990	Sep 1998	B-09-1998	Nov 2005	B-13-2005
Feb 1991	B-03-1991	Sep 1998	P-244	Feb 2006	B-02-2006
May 1991	B-07-1991	Sep 1998	P-244	May 2006	B-04-2006
Sep 1991	A-12-1991	Sep 1998	P-244	Sep 2006	D-311
Nov 1991	B-14-1991	Oct 1998	PS-52	Nov 2006	A-11-2006
Feb 1992	B-02-1992	Nov 1998	B-12-1998	Feb 2007	B-03-2007
May 1992	B-07-1992	Feb 1999	B-02-1999	May 2007	B-08-2007
Sep 1992	A-08-1992	May 1999	B-07-1999	July 2007	MSM-05-4
Sep 1992	B-14-1992	Aug 1999	A-10-1999	Aug 2007	B-11-2007
Oct 1992	B-16-1992	Sep 1999	B-13-1999	Nov 2007	A-14-2007
Feb 1993	B-02-2003	Nov 1999	B-16-1999	Feb 2008	A-01-2008
May 1993	B-07-1993	Feb 2000	B-02-2000	May 2008	B-08-2008
Aug 1993	A-14-1993	May 2000	B-06-2000	Aug 2008	A-11-2008
Sep 1993	B-11-1993	Aug 2000	B-10-2000	Oct 2008	KN-194
Oct 1993	B-14-1993	Nov 2000	B-14-2000	Nov 2008	A-13-2008
Feb 1994	B-03-1994	Feb 2001	B-02-2001	Feb 2009	B-01-2009
May 1994	B-08-1994	May 2001	B-06-2001	May 2009	B-05-2009
Sep 1994	B-14-1994	Aug 2001	B-10-2001	June 2009	MSM-12-1
Oct 1994	B-17-1994	Nov 2001	B-14-2001	Aug 2009	B-10-2009
Mar 1995	B-03-1995	May 2002	B-05-2002	Nov 2009	A-14-2009
May 1995	B-07-1995	Aug 2002	B-09-2002	Feb 2010	B-04-2010
Aug 1995	A-11-1995	Sep 2002	P-294	May 2010	B-08-2012
Sep 1995	B-14-1995	Nov 2002	A-10-2002	July 2010	M-82-1
Nov 1995	B-17-1995	Feb 2003	A-02-2003	Aug 2010	B-12-2010
Feb 1996	B-03-1996	May 2003	A-09-2003	Feb 2011	B-01-2011
Aug 1996	A-11-1996	Aug 2003	B-03-2003	May 2011	B-04-2011
Oct 1996	A-14-1996	Sep 2003	P-303	Aug 2011	M-85-2
Feb 1997	B-03-1997	Nov 2003	B-10-2003	Aug 2011	KN-203
May 1997	B-06-1997	Feb 2004	B-01-2004	Dec 2011	B-10-2011
Aug 1997	A-14-1997	May 2004	B-05-2004	Feb 2012	B-02-2012
Aug 1997	AR-34	Nov 2004	B-15-2004	May 2012	B-05-2012
Sep 1997	AR-34	Feb 2005	B-02-2005	Jun 2012	MSM-21-1b
Sep 1997	B-10-1997	May 2005	B-06-2005	Jul 2012	JR-267
Nov 1997	B-15-1997	Aug 2005	A-09-2005	Aug 2012	P-437
Feb 1998	B-02-1998	Aug 2005	P-327	Aug 2012	B-09-2012

^aPart (a) contains identification information for the cruises listed in the "cruise" column of part (b).

In particular, a bolus needs to be weakly stratified (have N^2 values less than or equal to $2 \times 10^{-6} \text{ s}^{-2}$), extend at least 150 m above sill depth, and occupy at least 65% of the area of the lower trough (below the ledge). These criteria were developed in part to comply with the *Spall and Price* [1998] modeling study of DSOW, which describes boluses as 150–200 m tall and 30 km wide. The width of the lower trough is approximately 25 km. The number of boluses in the synoptic sections is not sensitive to the precise choice of constraints. Figure 4 shows an example of a section that captured a bolus versus one where no bolus was present. The difference in the vicinity of the trough is quite pronounced in that the bolus (delimited by the gray line) is very cold and vertically uniform, and the pycnocline above it is much stronger than the deep stratification in the nonbolus section. Note also the difference in height of the 27.8 kg/m^3 isopycnal that defines the top of the overflow layer.

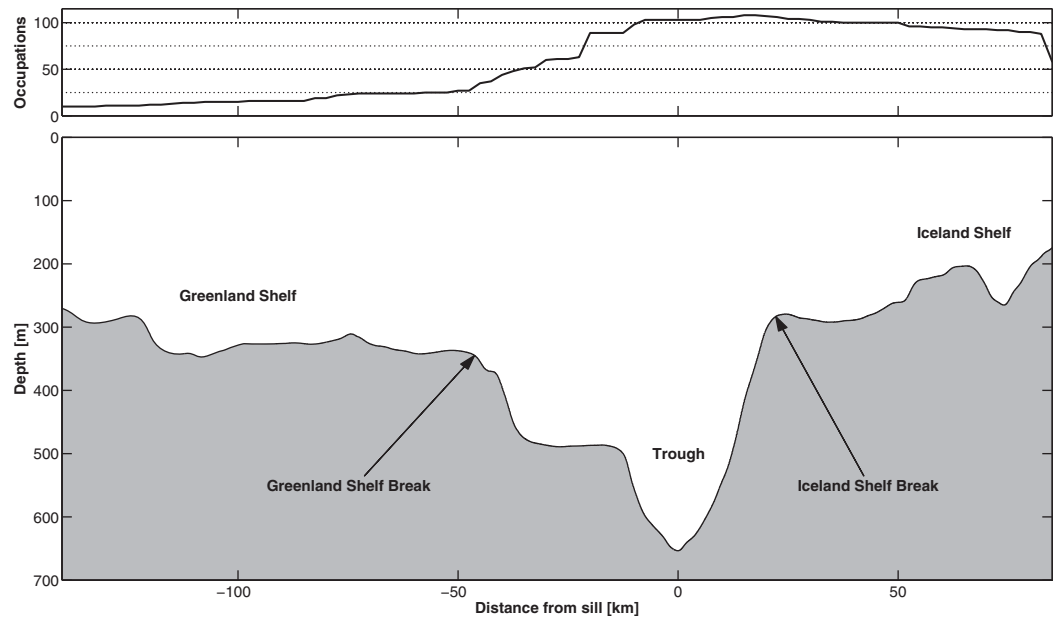


Figure 3. Bathymetry along the Látrabjarg line, with various topographic features identified. The upper plot indicates the data coverage of the vertical sections.

3. Results

3.1. Mean Hydrographic Conditions in Denmark Strait

Individual hydrographic sections occupied across Denmark Strait show the highly variable nature of the water masses passing over the sill. As such, it is difficult to discern persistent patterns in any given crossing. By averaging together many vertical sections, we are able to smooth out much of the synoptic variability, which reveals well-defined features across the strait. In turn, these features can be put in context of what is known about the water masses and currents upstream of the sill [e.g., *Våge et al., 2013; Harden et al., 2016*]. The mean potential temperature and salinity sections across the strait for the period 1990–2012 are shown in Figure 5, where in each case the mean potential density has been overlaid. (An earlier version of this figure appears in *von Appen et al. [2014b]*, but is only discussed briefly regarding a specific feature not considered in the present study.) We now describe the major features of the mean section and discuss the

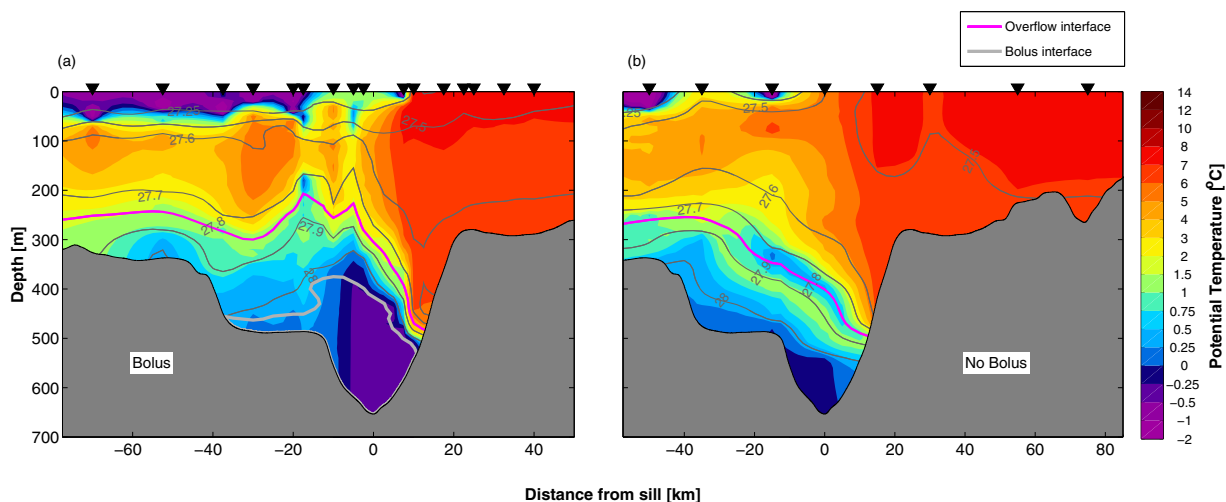


Figure 4. Two individual realizations of a vertical sections of potential temperature ($^{\circ}\text{C}$, color) overlain by potential density (kg/m^3 , contours) showing the (a) presence and (b) absence of a bolus of overflow water. The location of the bolus, based on the definition described in the text, is indicated by the gray line. The $27.8 \text{ kg}/\text{m}^3$ isopycnal is denoted by the magenta line. (a) Occupied June 2012 and (b) was occupied December 1997.

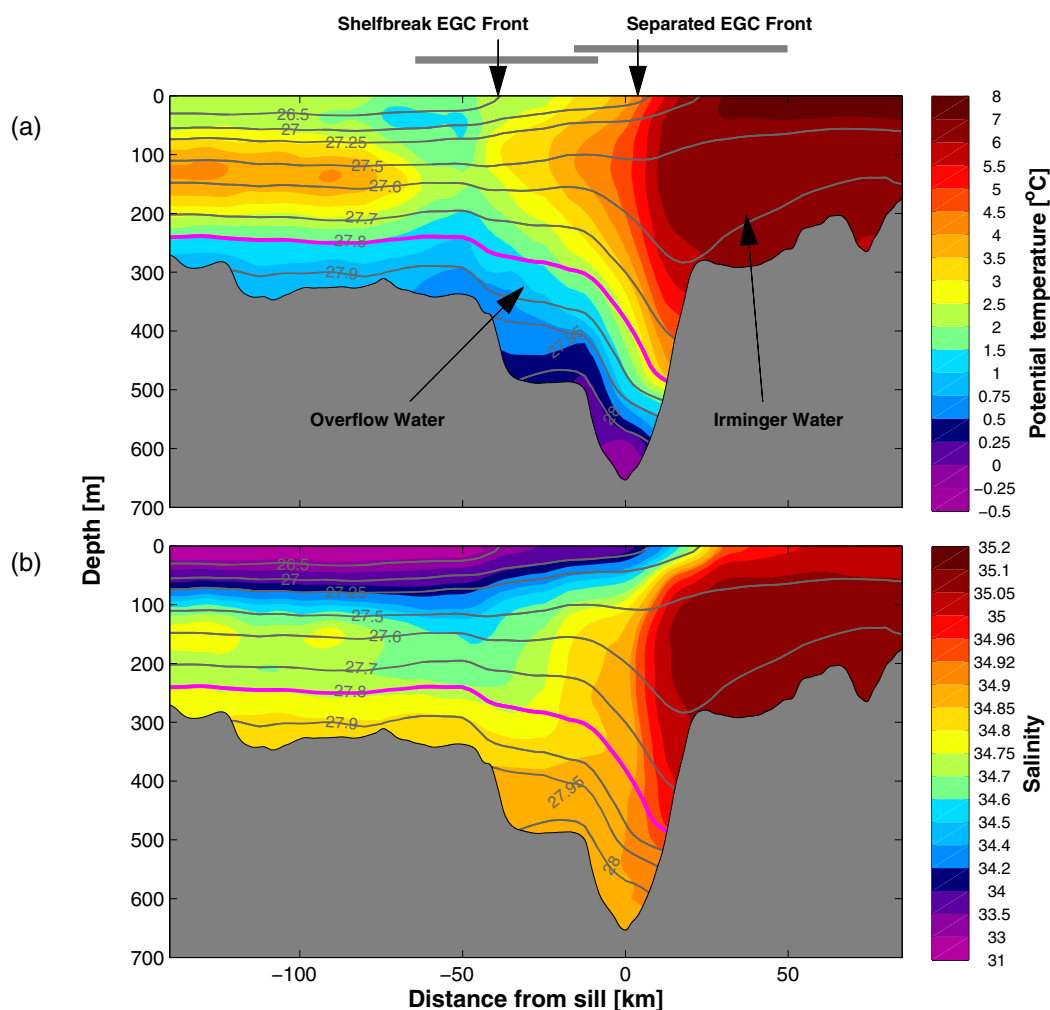


Figure 5. Mean vertical sections of (a) potential temperature ($^{\circ}\text{C}$, color) and (b) salinity (color), overlain by potential density (kg/m^3 , contours). The mean is comprised of data collected between 1990 and 2012. The $27.8 \text{ kg}/\text{m}^3$ isopycnal, which indicates the top of the overflow layer, is highlighted in magenta. The mean locations of the shelfbreak bars and separated EGC fronts are indicated by arrows at the top of the plot, and the corresponding ranges are indicated by horizontal gray bars.

seasonality as well as interannual trends in the water masses in the Strait. All reported trends are significant at the 95% confidence level.

The Iceland shelf is characterized by warm and salty water known as Irminger Water, which is subtropical in origin. This water mass is advected northward through the strait by the NIIC [Rudels *et al.*, 2002]. Our data reveal that the Irminger Water in Denmark Strait became warmer and saltier at a rate of 0.05°C and 0.005 per year, respectively, between 1990 and 2012. Seasonally, the Irminger Water is 1.8°C warmer during the summer and fall (June–November) compared to the winter and spring, with a maximum temperature in September. This value was determined by fitting a sinusoidal curve to the data. No statistically significant seasonality in salinity was detected. Both the seasonal and interannual changes in temperature of the Irminger Water at the Látrabjarg line are consistent with changes in this water mass observed farther north along the Iceland shelf [Jónsson and Valdimarsson, 2012]. In addition, Jónsson and Valdimarsson [2012] reported that the transport of the Irminger Water portion of the NIIC increased over the time period 1994–2010, and that it also varies seasonally with a maximum in summer and minimum in winter. We are not able to address the velocity characteristics of the NIIC at the Látrabjarg line because of the lack of velocity data there.

Farther to the west in the mean section there are two hydrographic fronts in the near surface layer: one is centered near 3 km and the other situated near the Greenland shelfbreak at roughly -44 km (indicated by

the two arrows in Figure 5). These are particularly evident in the mean salinity section. The latter front is associated with the shelfbreak EGC, and our mean section reveals that this current progresses southward through Denmark Strait. The former front coincides with the edge of the Irminger Water and is associated with the separated EGC, consistent with the mean upstream section across the Blosseville Basin presented by *Våge et al.* [2013]. Hence, both branches of the EGC are evident in the mean section—which is not the case in many of the synoptic crossings that contain small-scale features such as eddies or lenses of near-surface waters. For the transects where the two hydrographic fronts are clearly identifiable, the cross-strait range of the separated EGC front is 66 km whereas the shelfbreak EGC front is confined to a smaller range of 56 km (denoted by the gray lines in Figure 5). This discrepancy is to be expected, since the shelfbreak EGC is partially trapped to the shelfbreak while the separated EGC is more of a free jet. The locations of these fronts display neither seasonal nor interannual trends, and are reflective of synoptic variability.

Both the shelfbreak and separated EGC fronts are characterized by upward-sloping isopycnals from west to east (Figure 5). This is consistent with a surface-intensified southward flow of these two currents, in line with what is seen in the northern part of Denmark Strait [*Våge et al.*, 2013]. Deeper in the water column the isopycnals ($>27.5 \text{ kg/m}^3$) slope downward at these locations. This divergence in isopycnal slope implies that the deeper portions of the two currents are associated with enhanced southward flow of dense water over the sill. Upstream in the Blosseville Basin neither the shelfbreak EGC nor the separated EGC has such a reversal in isopycnal slope above sill depth. Perhaps this increased deep flow is related to the aspiration process that occurs in Denmark Strait [see *Harden et al.*, 2016]. Another complicating factor is that the NIJ advects overflow water into Denmark Strait in addition to the EGC [*Våge et al.*, 2013; *Harden et al.*, 2016]. In fact, *Harden et al.* [2016] demonstrated that, at the Kögur section roughly 220 km upstream of the sill, the separated EGC and NIJ are in the process of merging. Hence, the sloped isopycnals in the trough of Denmark Strait likely reflect the combined flow of these two currents.

At the western end of the mean section, shallower than roughly 75 m, relatively cold and fresh water is found on the Greenland shelf. According to the year-long mooring data set collected along the Kögur section, this water should also be flowing southward, although inshore of the core of the shelfbreak EGC [*Harden et al.*, 2016]. Recently *Håvik et al.* (personal communication, 2016) reported the presence of a freshwater jet on the Greenland shelf using a collection of hydrographic sections occupied between Fram Strait and Denmark Strait. The lack of any isopycnal slope in this part of our mean section, plus the fact that our data do not extend to the inner Greenland shelf, imply that we did not capture this feature. The seasonality of this water is such that it becomes warmer (by approximately 4°C) and fresher (by 0.8) during the summer and fall. This is consistent with the seasonal signal observed at the Kögur mooring array (*de Steur et al.*, personal communication, 2016). There was no statistically significant interannual trend of this upper-layer shelf water in our collection of sections.

The final feature of note in the mean Látrabjarg sections is an isolated region of warm, salty water in the depth range of 100–200 m on the Greenland shelf, from roughly -70 km to the western end of the section. This is modified Irminger Water that originated from the NIIC or the Irminger Current farther south, and subsequently mixed with surrounding water making it colder and fresher than the water on the Iceland shelf. It is well known that a significant portion of the Irminger Current retroflects in the vicinity of Denmark Strait [*Rudels et al.*, 2002]. Whether this split occurs north or south of the Látrabjarg line (or varies between the two scenarios) is presently unknown, and since we have no velocity information to accompany the property sections, we are unable to shed further light on this.

As seen in Figure 2, our data set contains occupations of the Látrabjarg line during all seasons, and so we created seasonal composite sections (not shown). However, aside from the above mentioned seasonality of the water on the Iceland and Greenland shelves, there was no significant variation over the remaining portion of the section. This may be due to the reduced number of sections in each season, but, based on previous studies using mooring data, there is no indication of seasonality of the overflow water [*Dickson and Brown*, 1994; *Jónsson*, 1999; *Jochumsen et al.*, 2012].

3.2. Water Mass Constituents in Denmark Strait

As noted above, north of Denmark Strait the two branches of the EGC advect Atlantic-Origin Overflow Water equatorward, while the NIJ advects Arctic-Origin Overflow Water equatorward. (This naming convention was established in the historical literature [e.g., *Swift and Aagaard*, 1981], and we adopt it here.) Due to

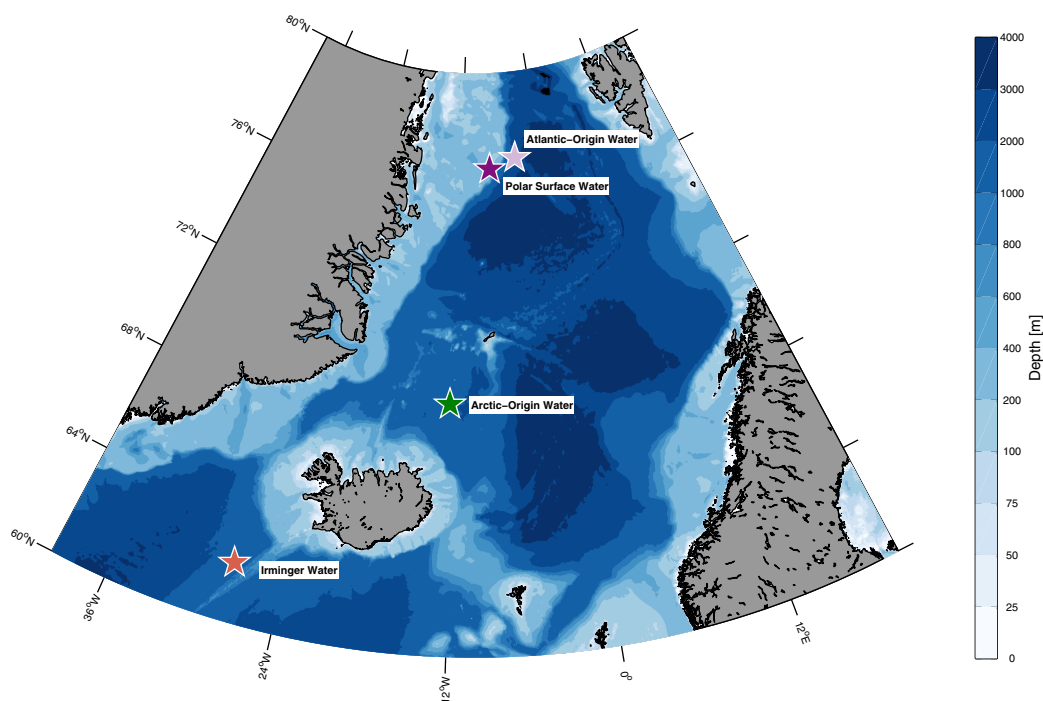


Figure 6. Locations where the end-member hydrographic T/S data were obtained (see text for details).

the lateral constriction of the strait, these currents are in close proximity to each other as they cross the sill, and the separated EGC and NIJ have likely merged. Consequently, it is not clear from the mean temperature and salinity sections of Figure 5 what the composition of overflow water masses is across the strait. We now investigate this using an end-member analysis.

3.3. Source Waters

We define four different water types as end-members for our calculation: Arctic-Origin Water, Atlantic-Origin Water, Irminger Water, and Polar Surface Water. Figure 6 shows the geographical areas from where we obtained data to determine the temperature/salinity (T/S) values of the end-members. These regions are sufficiently far away from the strait to result in a meaningful calculation. The locations for the Atlantic-Origin Water, Polar Surface Water, and Irminger Water—all within boundary currents—were determined based on high-resolution vertical sections in these areas. All reported trends in the end-member values are significant at the 95% level.

3.3.1. Arctic-Origin Water

Våge *et al.* [2011] argue that the source waters of the NIJ come from the region of the Iceland Sea. The water is presumably formed during convection in the winter months. However, wintertime hydrographic measurements in this region are very sparse [Våge *et al.*, 2015], making it difficult to define a robust end-member with such limited data. Hence, we used data from 567 hydrographic casts from the Iceland Sea over all months of the year between 1980 and 2013 from the historical data set described in section 2.2, and computed a mean T/S value for the depth range of 650–1000 m [extending well below sill depth to account for aspiration, Harden *et al.*, 2016]. The idea is to use an extreme value for the end-member, near the edge of the range of data at the strait. The resulting end-member index from this calculation is $-0.63 \pm 0.08^\circ\text{C}$ and 34.92 ± 0.01 (green star in Figure 7, where the box represents the standard deviation). There was no seasonality in either temperature or salinity of the end-member, but there was a small yet significant increase in temperature of 0.004°C per year.

3.3.2. Atlantic-Origin Water

The Atlantic-Origin Water end-member was also computed using the Nordic Seas historical database. We used all stations within a 100 km radius of the magenta star in Figure 6, resulting in a total of 451 casts from 1981 to 2012. The T/S value at the subsurface salinity maximum of this water mass was used, which

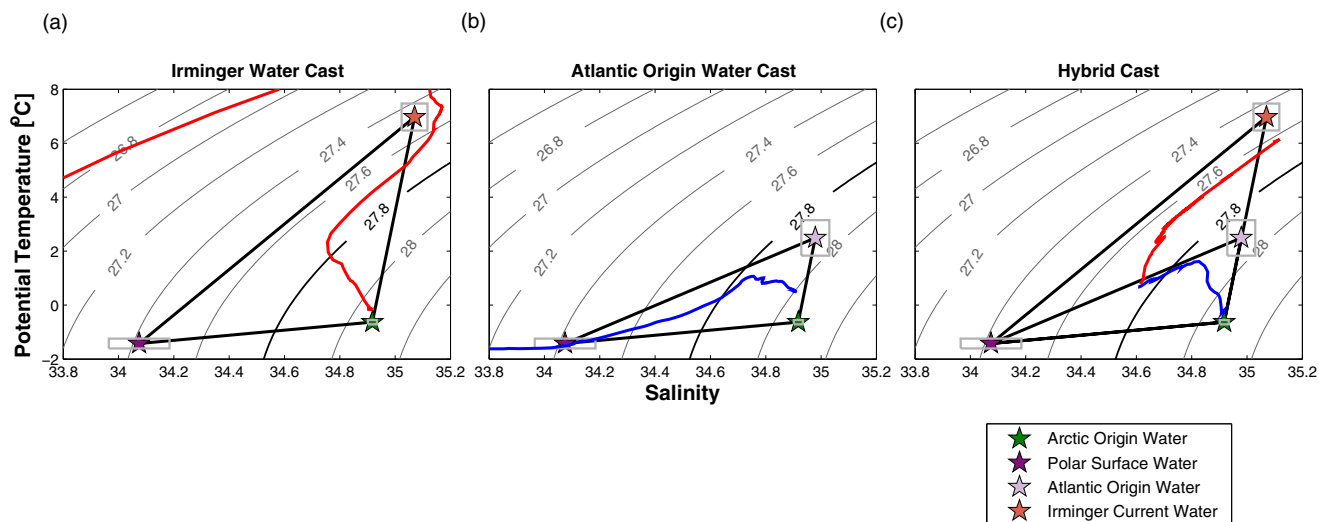


Figure 7. Examples of the three classes of CTD profiles found in Denmark Strait as they relate to the end-member analysis. (a) A cast that requires the Irminger Water mixing triangle; (b) a cast that requires the Atlantic-origin mixing triangle; and (c) a cast that requires both mixing triangles. The end-members are denoted by the stars (see the legend) and their standard deviations are denoted by gray boxes. The CTD casts are drawn in color. Red corresponds to data containing Irminger Water and blue corresponds to data containing Atlantic-Origin Water. The isopycnals are drawn using gray lines, and the 27.8 kg/m³ isopycnal is highlighted by the solid black line.

corresponds to the core of the shelfbreak EGC near 200 m depth. The resulting index is $2.50 \pm 0.66^\circ\text{C}$ and 34.98 ± 0.05 (magenta star in Figure 7). The Atlantic-Origin Water became warmer and saltier by 0.03°C and 0.002 per year, respectively, over the period of data coverage. The temperature of this end-member also varies seasonally, warming by roughly 1°C during summer/fall.

We note that the hydrographic properties of the Atlantic-Origin Water are continually modified via mixing in the boundary current around the Nordic Seas, hence it is somewhat arbitrary how far upstream one should go to compute this end-member. If the upstream distance was too great (e.g., where the Atlantic water enters the Norwegian Sea near the Faroe-Shetland Channel), then it would be difficult to distinguish this value from the Irminger Water entering the Iceland Sea in the NIIC. Our choice thus represents a balance between being too close versus too far from Denmark Strait.

3.3.3. Irminger Water

The end-member for this water mass was computed using the database covering the full North Atlantic Ocean (see section 2.2), where we used all casts within a 100 km radius of the orange star in Figure 6. As was the case for the Atlantic-Origin Water, we chose the T/S value corresponding to the salinity maximum of the current (roughly 200 m depth in the core of the Irminger Current). The associated end-member index is $6.97 \pm 0.50^\circ\text{C}$ and 35.07 ± 0.05 . Compared to the other end-members, the Irminger Water index was calculated using fewer casts (84) over a shorter time span (1987–2002) due to less data availability. This end-member warmed 0.07°C per year over this time period; however, no significant interannual trends in salinity were found. The Irminger Water also varies seasonally in temperature over a range of approximately 1.5°C , being warmest in September.

3.3.4. Polar Surface Water

The final end-member, Polar Surface Water, was computed at roughly the same distance upstream of Denmark Strait as the Atlantic-Origin Water using the Nordic Seas database. There were 200 casts occupied between 1981 and 2012 within a 100 km radius of the purple star in Figure 6. The T/S value corresponding to the temperature minimum in the depth range above the Atlantic layer and below the near-surface layer (approximately 50–100 m) was used. The resulting index is $-1.42 \pm 0.18^\circ\text{C}$ and 34.07 ± 0.11 . The temperature of the Polar Surface Water decreased by 0.008°C per year over the length of the record, but the salinity remained constant. The data suggest that this end-member may be warmer and fresher in the fall, but there are no measurements from December to April and therefore a seasonal signal cannot be determined with any certainty.

3.4. Mixing Triangles

The percent contribution of end-members to a given parcel of water can only be solved for three end-members [Mamayev, 1975]. Consequently, we defined two mixing triangles using the four end-members

described above, which were sufficient to characterize the waters across Denmark Strait. The two mixing triangles are (a) Arctic-Origin Water, Polar Surface Water, and Irminger Water; and (b) Arctic-Origin Water, Polar Surface Water, and Atlantic-Origin Water (see Figure 7). The assumption here is that, to leading order, the Irminger Water and Atlantic-Origin Water do not mix. This is reasonable since the Atlantic-Origin Water approaches Denmark Strait predominantly along the East Greenland continental slope at deeper levels than the Irminger Water, which resides mostly on the Iceland shelf and shelfbreak. Our assumption is obviously less valid for the recirculated Irminger Water, but the results presented below suggest that it still holds to a reasonable degree.

The calculation was carried out as follows. For each section, the individual casts were separated into three classes: those associated with mixing triangle (a), those associated with mixing triangle (b), and “hybrid” casts where part of the water column was characterized by (a) and part was characterized by (b). An example of each type of cast is shown in Figure 7. Profiles belonging to the first two classes were straightforward to identify as they had distinctly different curvatures in T/S space (see the examples of Figures 7a and 7b). These stations were located mostly on the eastern and western sides of the strait, respectively. For the remaining casts a semi-objective method was employed to determine where in the water column the transition occurred between the two regimes. In general this corresponded to a local maximum in the contribution of Polar Surface Water, below which Atlantic-Origin Water contributed to the mixing, and above which Irminger Water contributed to the mixing (see Figure 7c). Some of the data fell outside both of the mixing triangles, namely the water in the upper layer on the east Greenland shelf and the near-surface layer across the entire section. These regions are influenced by solar heating and/or very low values of salinity due to ice melt or glacial run off. These portions of the hydrographic casts were excluded from our calculation. This data reduction sometimes led to interpolation issues. Consequently, 19 sections were excluded from the analysis.

3.5. Percent Distributions

To quantify the water mass constituents in Denmark Strait, percentages of the end-members for each cast of each section were computed according to *Mamayev* [1975]. These percentages were then interpolated onto the standard grid for each section using the same interpolation scheme described in section 2.3. The mean vertical section of water mass percentages for all the sections (excluding the 19 mentioned above) is shown in Figure 8. To quantify the uncertainty in the percentages due to the seasonal and interannual variability as well as the station-to-station variability in the T/S of the end-members documented above, the calculation was repeated 500 times. For each iteration, the thermohaline indices of the different end-members were randomly selected from their respective distributions based on the historical data (the standard deviations of which are depicted by the uncertainty boxes in Figure 7). The differences in the resulting percentages were tabulated, and each of them displayed a normal distribution which did not change with further iterations. The uncertainties presented below reflect a combination of the standard deviations of these differences as well as the standard error associated with the mean of the collection of vertical sections.

Starting first with the nonoverflow water (lighter than 27.8 kg/m^3) one sees that, as expected, the water on the Iceland shelf is nearly 100% Irminger Water. On the other hand, the water that has recirculated from the NIIC, shallower than 200 m and west of -60 km , is a mixture of roughly $64 \pm 3\%$ Irminger Water, $28 \pm 3\%$ Polar Surface Water, and $8 \pm 1\%$ Arctic-Origin Water. Polar Surface Water is present westward of the trough in significant amounts, with the highest percentage (approximately $60 \pm 8\%$) in the region between the NIIC and the recirculated Irminger Water.

The most enlightening aspect of the mixing calculation pertains to the DSOW. The deepest part of the trough is dominated by Arctic-Origin Water (approaching 100%), although there is a nontrivial percentage of Irminger Water that gets entrained into the overflow on the eastern side of the trough ($8 \pm 1\%$). This is consistent with the upstream observations showing that the densest portion of the overflow is supplied by the NIJ [*Våge et al.*, 2011; *Harden et al.*, 2016]. Progressing to the west, one sees that the highest percentage of Atlantic-Origin Water is found in the vicinity of the East Greenland shelfbreak and above the ledge, likely transported there by the shelfbreak EGC. However, the maximum percentage is only $72 \pm 9\%$, indicating that the component of DSOW carried by the EGC is more diluted by the time it reaches the sill than much of the NIJ water. Figure 8 demonstrates that both Polar Surface Water ($15 \pm 9\%$) and Arctic-Origin Water

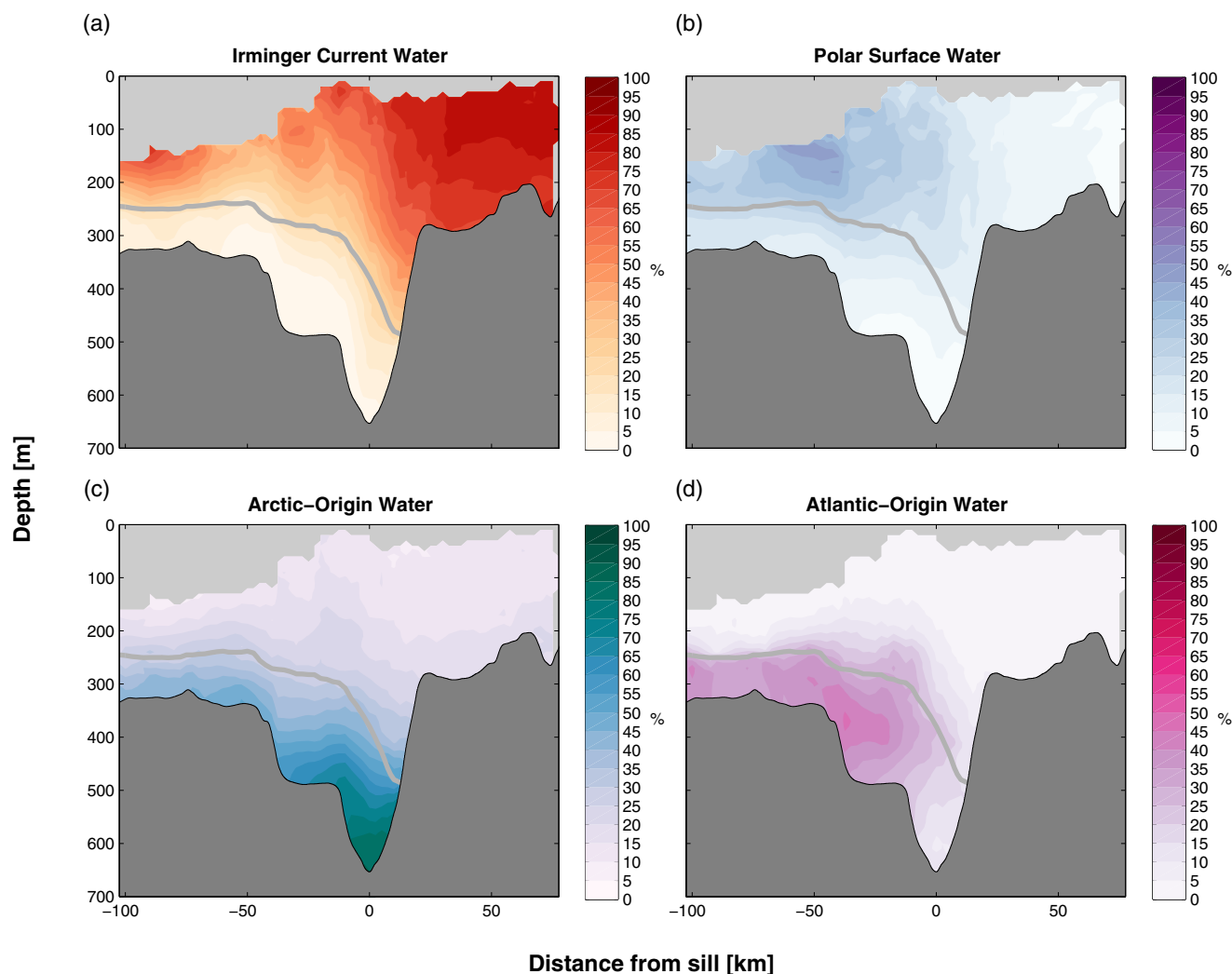


Figure 8. Vertical sections of the mean percent contributions of the end-member water masses. (a) Irminger Water; (b) Polar Surface Water; (c) Arctic-Origin Water; and (d) Atlantic-Origin Water. The 27.8 kg/m^3 isopycnal is denoted by the gray line.

($14 \pm 9\%$) mix with the Atlantic-Origin Water. Notably, the DSOW residing on the east Greenland shelf also contains appreciable amounts of these other water types.

There are several possible explanations as to why Arctic-Origin Overflow Water is found in appreciable quantities on the western side of Denmark Strait. First, a portion of the NIJ likely transposes from the Iceland slope to the Greenland slope as it approaches the sill. This is to be expected based on geostrophic control (i.e., the “dam break” problem for dense water) as well as hydraulic theory [Gill, 1976; Hermann and Rhines, 1989; Pratt and Whitehead, 2008]. Another possibility is that some of this dense water recirculates onto the Greenland shelf after it flows over the sill, which is in line with the model Lagrangian float tracks of Koszalka *et al.* [2013] and von Appen *et al.* [2014b]. Third, some of this water may aspirate from the deep layers of the EGC, which transports water with T/S properties almost identical to Arctic-Origin Overflow Water. While this deep water is typically found at depths greater than 850 m north of the sill, Harden *et al.* [2016] calculate that roughly 0.6 Sv of overflow water emanates from below sill depth.

It is important to note that our end-member percentages are not biased by the possibility that a portion of the Arctic-Origin Water emanates from outside of the Iceland Sea (where the end-member was calculated); dense water with these characteristics is found to the west and north, including the Greenland Sea. Regardless of the exact geographical origin of this end-member, our conclusions still hold: while the deep trough is dominated by Arctic-Origin Water with only negligible amounts of Atlantic-Origin Water, the DSOW on

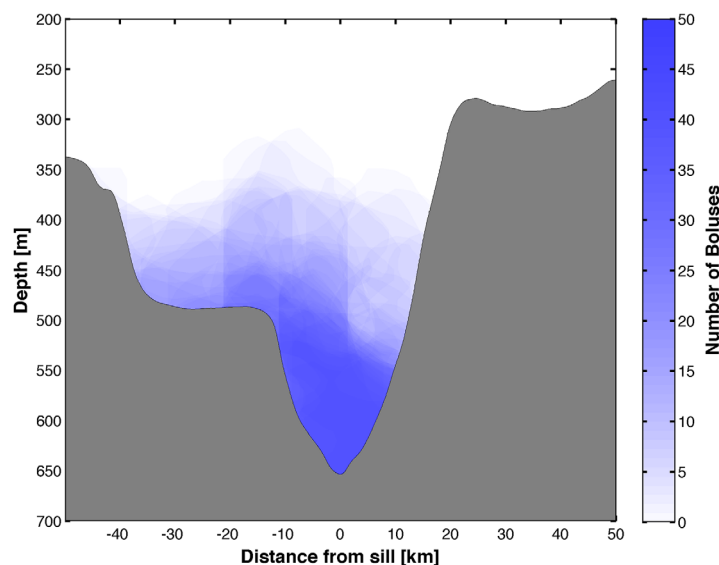


Figure 9. Overlays of the 46 boluses identified in the individual sections across Denmark Strait.

the western side of the strait—above the ledge and onto the Greenland shelf—is a mixture of both constituents, with a contribution from the Polar Surface Water.

3.6. Boluses in Denmark Strait

The most pronounced variation in the structure of the DSOW at the sill is due to the passage of boluses of overflow water. We now characterize the size, location, and hydrographic characteristics of the boluses using our collection of vertical sections. We then investigate the interannual trends in the hydrographic properties of the boluses and relate them to changes in the source waters.

According to our definition of a bolus (section 2.4), these features are present in 41% (46 of the 111) of the synoptic sections (Figure 2). There is no apparent seasonality to their occurrence. An example of a bolus was shown earlier in Figure 4 (compared to a nonbolus section). The bolus contains a large amount of water colder than -0.25°C occupying the deepest part of the trough, although the feature accounts for less than half of the overflow water present in the section. Overlaying all bolus occurrences (Figure 9) reveals that the majority of them are banked on the western side of the trough, which has been noted for individual hydrographic sections occupied across the sill [e.g., *Macrander et al.*, 2007] and is consistent with hydraulic theory [*Pratt and Whitehead*, 2008]. However, some are found on the eastern side, while some extend onto the ledge toward the Greenland shelfbreak. In nearly all cases they fill the deepest part of the trough.

Boluses constitute the coldest, saltiest, and densest portion of the DSOW. In particular, boluses are on average $0.049 \pm 0.003 \text{ kg/m}^3$ denser than the surrounding overflow water. They have an average cross-sectional area of $4.08 \pm 0.27 \text{ km}^2$. This value, however, slightly underestimates their true size, because a few sections stop short of fully resolving them. Boluses contain mostly Arctic-Origin Water, with only small amounts of the other end-member water masses. The mean end-member contributions for boluses are: $80 \pm 9\%$ Arctic-Origin Water; $14 \pm 9\%$ Atlantic-Origin Water; $4 \pm 3\%$ Polar Surface Water; and $2 \pm 2\%$ Irminger Water. By comparison, the mean end-member contributions of the remaining (nonbolus) DSOW are: $63 \pm 9\%$ Arctic-Origin Water; $23 \pm 9\%$ Atlantic-Origin Water; $8 \pm 3\%$ Polar Surface Water; and $6 \pm 1\%$ Irminger Water.

Although boluses do not exhibit seasonality, they have become warmer and saltier over the time period of our data set at a rate of 0.011°C and 0.0013 per year, respectively. The T/S changes generally compensate each other so that there has been no appreciable change in density. While these trends are small, they are significant at the 95% confidence level and are clearly visible in T/S space (Figure 10). This corresponds to a total change in temperature and salinity of 0.22°C and 0.026 , respectively, over 20 years (no boluses were detected in the first 2 years of the record). These changes are explainable by considering both the trends in end-member properties as well as their percentages.

As documented earlier, both the Arctic-Origin Water and Atlantic-Origin Water end-members have become warmer, which can explain part of the observed warming of the boluses. By contrast, only the Atlantic-Origin Water end-member has become saltier, but the rate of change is too small to account for the observed increase in bolus salinity. Regarding percentages, there has been a reduction in the contribution of the two freshest and coldest end-members (Arctic-Origin Water and Polar Surface Water) and an increase in the two that are saltiest and warmest (Atlantic-Origin Water and Irminger Water). While only the change in the Polar Surface Water percentage is significant at the 95% confidence level, we nonetheless calculated the predicted change in bolus properties due to all of the percent changes, in addition to the trends in the

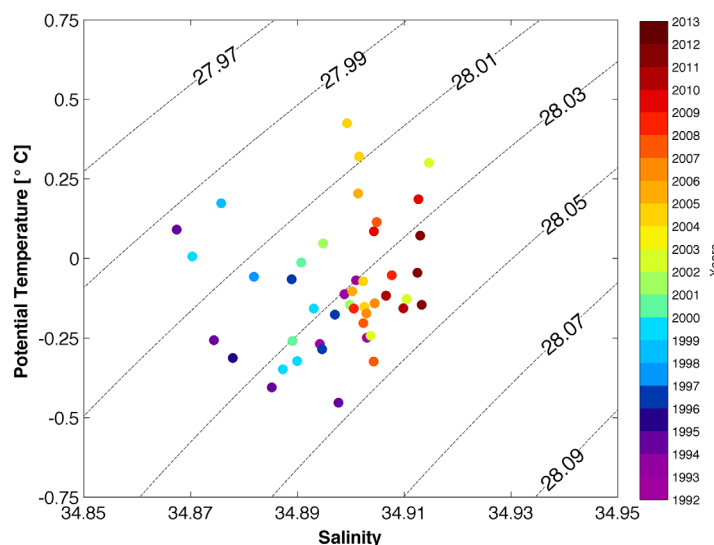


Figure 10. The temperature and salinity values of boluses versus time (years; color). Density is contoured in black. A very saline outlying bolus has been removed from the figure.

end-member T/S properties. The result—a warming of 0.36°C and salinization of 0.026 —agrees reasonably well with the measured change in bolus properties noted above.

4. Summary and Discussion

This study has investigated the hydrographic structure across the Denmark Strait sill using 111 shipboard sections occupied between 1990 and 2012, with an emphasis on the dense overflow water. By averaging out the synoptic variability in the individual transects, we have revealed the presence of the shelfbreak East Greenland Current (EGC) and the separated EGC, two of the main circulation components that exist upstream of the sill. The third upstream circulation feature, the North Icelandic Jet, appears to have merged with the deep portion of the separated EGC. The Iceland shelf is filled with warm and salty Irminger Water, while the mid-depth portion of the East Greenland shelf contains modified Irminger Water that presumably has recirculated from the North Icelandic Irminger Current.

In order to quantify the water mass structure at the sill we carried out an end-member analysis with four source waters: Arctic-Origin Water, Atlantic-Origin Water, Polar Surface Water, and Irminger Water. As expected, the Irminger Water is dominant on the Iceland shelf, and the Polar Surface Water is most prevalent on the Greenland shelf. With regards to the overflow water, the deepest part of the Denmark Strait trough is nearly all Arctic-Origin Water. To the west, in the vicinity of the Greenland shelfbreak, the overflow water is dominated by Atlantic-Origin Water, but there is also a significant amount of Polar Surface Water and Arctic-Origin Water. The presence of the latter water mass could be due to several factors, including partial transposition of the NIJ as it approaches the sill, recirculation of Arctic-Origin Water south of the sill, or aspiration from the deep layers of the EGC.

Large, cold, weakly stratified lenses of water called boluses were observed in 41% of the hydrographic transects. These features are predominantly banked on the western side of the deep trough, although they are occasionally found on the eastern side of the trough as well as above the ledge adjacent to the Greenland shelfbreak. The boluses are colder, saltier, and denser than the remaining overflow water, and are comprised mostly of Arctic-Origin Water which indicates that the boluses are supplied primarily by the NIJ [Våge *et al.*, 2011]. While there is no seasonality to the boluses, they have become warmer and saltier over the 22 year span of data coverage. This seems to be due to trends in the end-member T/S values in concert with changes in the percentage of these water mass constituents.

While our study has elucidated the hydrographic structure in Denmark Strait and has shed light on the characteristics of the boluses of overflow water that periodically pass through the strait, many questions remain to be answered. For example, the mean velocity field across the strait is unknown. While it is evident that the two hydrographic fronts revealed here correspond to the shelfbreak EGC and separated EGC, their kinematic structures and transports need to be determined. Furthermore, the geostrophic shear in these regions of the strait—in particular the near-bottom reversal in shear—needs to be reconciled with the upstream structure of these two currents presented in Harden *et al.* [2016]. This will help us understand the flow adjustments that take place as the water approaches the sill. Additional work is also required to understand the precise origin of the boluses. Toward this end it would be enlightening to conduct a multivariate analysis of transient tracers, along the lines of that carried out by Tanhua *et al.* [2005]. Finally, the downstream

fate of the boluses needs to be further explored. von Appen et al. (personal communication, 2016) argue that they lead to the formation of DSOW cyclones that are commonly observed along the western boundary of the Irminger Sea. If true, then the boluses play a significant role in the entrainment and mixing that occurs south of the sill which helps dictate the final properties of North Atlantic Deep Water.

Acknowledgments

The authors acknowledge Carolina Nobre for help with programming and constructing figures, and Ben Harden for sharing the interpolation scheme for gridding the shipboard sections. Thanks are extended to Bert Rudels and Gerd Krahnmann for contributing hydrographic data. Support for the project was provided by the following sources: the US National Science Foundation (RP and DM) via grant OCE-0959381; the Norwegian Research Council under grant 231647 (KV); the Bergen Research Foundation (KV); the European Union 7th Framework Program (FP7 2007-2013) under grant 308299 (NACLIM project, KV and KJ) and grant GA212643 (THOR project, KJ); the Cooperative project "RACE—Regional Atlantic Circulation and Global Change" funded by the German Federal Ministry for Education and Research (BMBF), 03f0651a (KJ). The shipboard transect data used in the study are available at kogur.whoi.edu.

References

- Bruce, J. (1995), Eddies southwest of the Denmark Strait, *Deep Sea Res., Part I*, 42(1), 13–29, doi:10.1016/0967-0637(94)00040-y.
- Cooper, L. H. N. (1955), Deep water movements in the North Atlantic as a link between climatic changes around Iceland and biological productivity of the English Channel and Celtic Sea, *J. Mar. Res.*, 14, 347–362.
- Dickson, R., and J. Brown (1994), The production of North Atlantic Deep Water: Sources, rates, and pathways, *J. Geophys. Res.*, 99(C6), 12,319–12,341, doi:10.1029/94JC00530.
- Dickson, R. R., J. Meincke, and P. B. Rhines (2008), *Arctic-Subarctic Ocean Fluxes*, Springer, Dordrecht, Netherlands.
- Fristedt, T., R. Hietala, and P. Lundberg (1999), Stability properties of a barotropic surface-water jet observed in the Denmark Strait, *Tellus, Ser. A*, 51, 979–989, doi:10.3402/tellusa.v51i5.14506.
- Gill, A. (1976), Adjustment under gravity in a rotating channel, *J. Fluid Mech.*, 77(3), 603–621, doi:10.1017/s0022112076002280.
- Girton, J., and T. Sanford (2003), Descent and modification of the overflow plume in the Denmark Strait, *J. Phys. Oceanogr.*, 33(7), 1351–1364, doi:10.1175/1520-0485(2003)033<1351:DAMOTO>2.0.CO;2.
- Harden, B., R. Pickart, H. Valdimarsson, K. Våge, L. deSteuer, E. Børve, S. Jónsson, A. Macrander, and L. Håvik (2016), Upstream sources of the Denmark Strait Overflow: Observations from a high-resolution mooring array, *Deep Sea Res., Part I*, 112, 94–112, doi:10.1016/j.dsr.2016.02.007.
- Hermann, A., P. Rhines, and E. Johnson (1989), Nonlinear Rossby adjustment in a channel: Beyond Kelvin waves, *J. Fluid Mech.*, 205, 469–502, doi:10.1017/s0022112089002119.
- Jiang, L., and R. Garwood (1996), Three-dimensional simulations of overflows on continental slopes, *J. Phys. Oceanogr.*, 26(7), 1214–1233, doi:10.1175/1520-0485(1996)026<1214:TDSOOO>2.0.CO;2.
- Jochumsen, K., D. Quadfasel, H. Valdimarsson, and S. Jónsson (2012), Variability of the Denmark Strait overflow: Moored time series from 1996–2011, *J. Geophys. Res.*, 117, C12003, doi:10.1029/2012JC008244.
- Jónsson, S. (1999), The circulation in the northern part of the Denmark Strait and its variability, *ICES CM L:06*, 9 pp., ICES Journal of Marine Science, Copenhagen, Denmark.
- Jónsson, S., and H. Valdimarsson (2004), A new path for the Denmark Strait Overflow Water from the Iceland Sea to Denmark Strait, *Geophys. Res. Lett.*, 31, L03305, doi:10.1029/2003GL019214.
- Jungclauss, J., and J. Backhaus (1994), Application of a transient reduced gravity plume model to the Denmark Strait Overflow, *J. Geophys. Res.*, 99(C6), 12,375–12,396, doi:10.1029/94JC00528.
- Käse, R., and A. Oschlies (2000), Flow through Denmark Strait, *J. Geophys. Res.*, 105(C12), 28,527–28,546, doi:10.1029/2000JC00111.
- Käse, R., J. B. Girton, and T. B. Sanford (2003), Structure and variability of the Denmark Strait Overflow: Model and observations, *J. Geophys. Res.*, 108(C6), 3181, doi:10.1029/2002JC001548.
- Koszalka, M., I. T. Haine, and M. Magaldi (2013), Fates and travel times of Denmark Strait Overflow Water in the Irminger Basin, *J. Phys. Oceanogr.*, 43(12), 2611–2628, doi:10.1175/jpo-d-13-023.1.
- Krauss, W. (1996), A note on overflow eddies, *Deep Sea Res., Part I*, 43(10), 1661–1667, doi:10.1016/s0967-0637(96)00073-8.
- Krauss, W., and R. Käse (1998), Eddy formation in the Denmark Strait overflow, *J. Geophys. Res.*, 103(C8), 15,525–15,538, doi:10.1029/98JC00785.
- Macrander, A., R. Käse, U. Send, H. Valdimarsson, and S. Jónsson (2007), Spatial and temporal structure of the Denmark Strait Overflow revealed by acoustic observations, *Ocean Dyn.*, 57, 75–89, doi:10.1007/s10236-007-0101-x.
- Magaldi, M., T. Haine, and R. Pickart (2011), On the nature and variability of the East Greenland spill jet: A case study in summer 2003, *J. Phys. Oceanogr.*, 41(12), 2307–2327, doi:10.1175/jpo-d-10-05004.1.
- Mamayev, O. (1975), *Temperature-Salinity Analysis of World Ocean Waters*, Elsevier Sci., Amsterdam.
- Mastropole, D. (2015), Hydrographic structure of overflow water passing through the Denmark Strait, MS, MIT and Woods Hole Oceanogr. Inst., Woods Hole, Mass. [Available at <http://dspace.mit.edu/handle/1721.1/7582>.]
- Mauritzen, C. (1996), Production of dense overflow waters feeding the North Atlantic across the Greenland-Scotland Ridge. Part 1: Evidence for a revised circulation scheme, *Deep Sea Res., Part I*, 43(6), 769–806, doi:10.1016/0967-0637(96)00037-4.
- Nikolopoulos, A., K. Borenäs, R. Hietala, and P. Lundberg (2003), Hydraulic estimates of Denmark Strait overflow, *J. Geophys. Res.*, 108(C3), 3095, doi:10.1029/2001JC001283.
- Paquette, R., R. Bourke, J. Newton, and W. Perdue (1985), The East Greenland Polar Front in autumn, *J. Geophys. Res.*, 90(C3), 4866–4882, doi:10.1029/JC090iC03p04866.
- Pratt, L., and J. Whitehead (2008), *Rotating Hydraulics—Nonlinear Topographic Effects in the Ocean and Atmosphere*, Springer, New York.
- Price, J. F., and M. O’Neil Baringer (1994), Outflows and deep water production by marginal seas, *Prog. Oceanogr.*, 33(3), 161–200, doi:10.1016/0079-6611(94)90027-2.
- Rudels, B., P. Eriksson, H. Grönvall, R. Hietala, and J. Launiainen (1999), Hydrographic observations in Denmark Strait in fall 1997, and their implications for the entrainment into the overflow plume, *Geophys. Res. Lett.*, 26(9), 1325–1328, doi:10.1029/1999GL900212.
- Rudels, B., E. Fahrbach, J. Meincke, G. Budeus, and P. Eriksson (2002), The East Greenland Current and its contribution to the Denmark Strait overflow, *ICES J. Mar. Sci.*, 59(6), 1133–1154, doi:10.1006/jmsc.2002.1284.
- Shi, X., L. Røed, and B. Hackett (2001), Variability of the Denmark Strait overflow: A numerical study, *J. Geophys. Res.*, 106(C10), 22,277–22,294, doi:10.1029/2000JC000642.
- Smith, P. (1975), A streamtube model for bottom boundary currents in the ocean, *Deep Sea Res., Oceanogr. Abstr.*, 22(12), 853–873, doi:10.1016/0011-7471(75)90088-1.
- Smith, P. (1976), Baroclinic instability in the Denmark Strait overflow, *J. Phys. Oceanogr.*, 6(3), 355–371, doi:10.1175/1520-0485(1976)006<0355:BIITDS>2.0.CO;2.
- Smith, W., and P. Wessel (1990), Gridding with continuous curvature splines in tension, *Geophysics*, 55(3), 293–305, doi:10.1190/1.1442837.
- Spall, M., and J. Price (1998), Mesoscale variability in Denmark Strait: The PV outflow hypothesis, *J. Phys. Oceanogr.*, 28(8), 1598–1623, doi:10.1175/1520-0485(1998)028<1598:MVIDST>2.0.CO;2.

- Swift, J. and K. Aagaard (1981), Seasonal transitions and water mass formation in the Iceland and Greenland seas, *Deep Sea Res. Part A Oceanogr. Res. Pap.*, 28, 1107–1129, doi:10.1016/0198-0149(81)90050-9.
- Tanhua, T., K. Olsson, and E. Jeansson (2005), Formation of Denmark Strait Overflow Water and its hydro-chemical composition, *J. Mar. Syst.*, 57(3–4), 264–288, doi:10.1016/j.jmarsys.2005.05.003.
- von Appen, W., R. Pickart, K. Brink, and T. Haine (2014a), Water column structure and statistics of Denmark Strait Overflow Water cyclones, *Deep Sea Res., Part I*, 84, 110–126, doi:10.1016/j.dsr.2013.10.007.
- von Appen, W., I. Koszalka, R. Pickart, T. Haine, D. Mastropole, M. Magaldi, H. Valdimarsson, J. Girton, K. Jochumsen, and G. Krahnmann (2014b), The East Greenland Spill Jet as an important component of the Atlantic Meridional Overturning Circulation, *Deep Sea Res., Part I*, 92, 75–84, doi:10.1016/j.dsr.2014.06.002.
- Våge, K., R. Pickart, M. Spall, H. Valdimarsson, S. Jónsson, D. Torres, S. Østerhus, and T. Eldevik (2011), Significant role of the North Icelandic Jet in the formation of Denmark Strait Overflow Water, *Nat. Geosci.*, 4(10), 723–727, doi:10.1038/ngeo1234.
- Våge, K., R. Pickart, M. Spall, G. Moore, H. Valdimarsson, D. Torres, S. Erofeeva, and J. Nilsen (2013), Revised circulation scheme north of the Denmark Strait, *Deep Sea Res., Part I*, 79, 20–39, doi:10.1016/j.dsr.2013.05.007.
- Våge, K., G. W. K. Moore, S. Jónsson, and H. Valdimarsson (2015), Water mass transformation in the Iceland Sea, *Deep Sea Res., Part I*, 101, 98–109, doi:10.1016/j.dsr.2015.04.001.
- Worthington, L. V. (1969), An attempt to measure the volume transport of Norwegian Sea overflow water through the Denmark Strait, *Deep Sea Res., Oceanogr. Abstr.*, 16, suppl., 421–432.